Magnesium Technology 2011
Edited by: Wim H. Sillekens, Sean R. Agnew, Neale R. Neelameggham, and Suveen N. Mathaudhu
TMS (The Minerals, Metals & Materials Society), 2011

MAGNESIUM ALLOYS FOR BIOABSORBABLE STENTS: A FEASIBILITY ASSESSMENT

Charles Z. Deng[1], Rajesh Radhakrishnan[1], Steve R. Larsen[1], Dennis A. Boismer[1], Jon S. Stinson[1], Adrienne K. Hotchkiss[1], Eric M. Petersen[1], Jan Weber[2], and Torsten Scheuermann[3]

[1]Boston Scientific Inc., Maple Grove, Minnesota, USA
[2]Boston Scientific, Maastricht, The Netherlands
[3]Boston Scientific Technology Center GmbH, Munich, Germany

Keywords: magnesium, stent, bioabsorbable

Abstract

Today, stent designs consist of permanent metal alloy scaffolds which hold arteries open after percutaneous coronary intervention (PCI) to maintain arterial blood flow. Bioabsorbable stents are being investigated as an alternate for permanent stents, that disintegrate and dissolve in the body. In this article, we profile magnesium (Mg) alloy as a candidate for bioabsorbable stent material, and discuss aspects of its properties and challenges. Experimental data are generated in effort to draw correlations between in vivo vessel absorption and in vitro degradation, and to provide an overview of alloy mechanical properties, stent designs, and electrochemical behaviors. Preclinical porcine coronary model test results exhibit early on-set and rapid corrosion presenting a challenge to researchers to establish material design concepts that balance degradation time, duration for need of scaffolding, and healing.

Introduction

Cardiovascular disease is the leading cause of death in the world. Millions of people undergo PCI every year to treat the many varieties of vascular disease. Most often, the therapies utilized include the placement of a permanent stent implant to keep arteries open after the procedure. Over the past several years, many researchers in industry and academia have been exploring the concept of an absorbable stent that goes away over time [1-6].

Potential benefits of absorbable stents include cessation or elimination of antiplatelet therapies that complicate the necessity for the treatment of other medical conditions the patients require - adding risk to the overall health. Other benefits are possible including restoration of vessel properties such as vasomotion which is the ability for the vessel to expand and contract as the body attempts to modulate blood flow between times of rest and exercise. Additionally, absorbable stents would likely create the ability to more efficiently treat a previously stented site, or to enable the option of a bypass graft without the hindrance of an existing implant. Absorbable stents may also be used successfully as a way to deliver anti-restenosis drugs such as Everolimus or Paclitaxel.

Metal stents made of magnesium alloy have been studied for several years in animals [7-10] and humans [11-13] with reportedly encouraging results in terms of strength and degradation time. However there are many complexities associated with engineering the stent that range from its basic strength, biocompatibility, healing response, and rate of absorption. Of fundamental concern are the many interactive biological, chemical, and metallurgical mechanisms that dictate how these metal stents dissolve in the body and the yet to be discovered pathways of how the body responds to the material and its corrosion induced by-products.

Scope of this study was the evaluation of different magnesium alloys and coatings to gain knowledge about their corrosion rates and modes in animals and its predictability through bench tests.

Assessments

Design of absorbable stent

Magnesium alloys have generated a significant increase in interest from researchers in the search for biodegradable implant materials [14-30]. The design criteria for a magnesium stent challenge conventional permanent stent implant thinking due to its relatively low modulus, low ductility, and high corrosion rate. The stent must function mechanically for basic design performance such as radial strength and deliverability, and must compete in the marketplace not just with current stents available, but with next generation stents in the next 5-10 years. Starting a priori from a thin design (less than 100 micrometer strut thickness) in combination with a minimum corrosion period of at least 3-6 months so as to allow encapsulation in the neointima while providing sufficient radial force against elastic recoil, leads to the realization that many commercially available magnesium alloys are not compatible with stent design criteria, forces one to consider new alloys and a protective coating to be used in the design. The protective coating itself should be thin, pinhole free and robust, not only to avoid adding overall stent thickness, but also to withstand deformations occurring during assembly, delivery, and expansion of the stent. Figure 1 demonstrates the technical feasibility of such a coating.

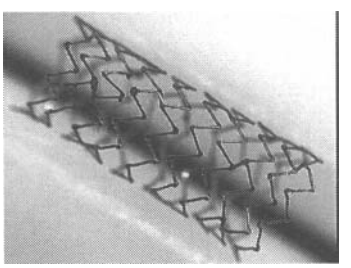

Figure 1. A thin coated magnesium alloy stent immersed in simulated body fluid for 4 weeks at 37°C showed little corrosion and remained intact, while uncoated stents only remained intact for a few days.

Additionally, the stent must be biocompatible, and the luminal surface should permit rapid endothelialization and should be compatible with anti-restenotic drugs eluting from the stent. A too rapid corrosion process in later phases can result in a deposition of large amounts of magnesium phosphate as shown in the left of Figure 2. The magnesium phosphate may in fact simply replace

the initial magnesium volume, beating the overall biodegradability. The right image in Figure 2 is a slow corroding MZX, a non-commercial alloy covered by magnesium hydroxide coating and tissue.

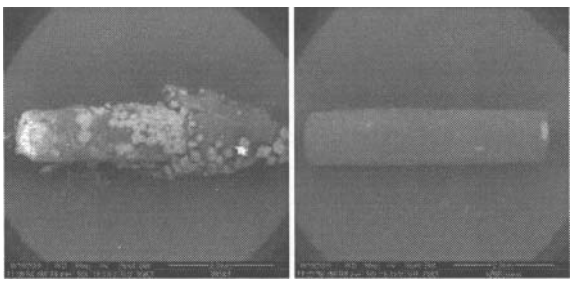

Figure 2. Explanted bare magnesium rods (left–WE43, right–MZX, a non commercial alloy) from mouse subcutaneous implant in 1- month.

Mechanical properties

Tensile test data was generated for each of the magnesium alloys evaluated utilizing samples of annealed stent-sized tubing. Tensile tests were performed using parameters in general accordance with ASTM E8, "Standard Test Methods for Tensile Testing of Metallic Materials". Mandrels were inserted into the tube at the sample ends to aid gripping during the test which was performed on a Sintech 1 G load frame, with a grip separation of 76.2 mm and elongation to fracture was measured over 50.8 mm. Test speeds were ranged from 0.254-5.08 mm/min. A 50.8 mm gage length extensometer was used for measuring strain.

Table I presents average tensile test data for the annealed magnesium alloy tubing. The materials evaluated have a relatively narrow range in strength and ductility at levels which represent a challenge for stent design and performance. No significant strain rate effect was observed for any of the materials over the range of rates tested.

Table I. Tensile test data of annealed Mg alloy and 316L stainless steel tubing.

Material	Elastic Modulus (GPa)	0.2% Yield Strength (MPa)	Tensile Strength (MPa)	Elongation (%)
316L SS	193	275	595	50
WE43B	43	169	254	18
ZK31	45	223	287	13
AZ80	43	163	255	7
MZX*	43-46	165-203	265-308	8-23

* MZX is a series of non commercial alloy which contains magnesium, zinc, and other elements.

Electrochemical properties

A survey of magnesium alloy bio-corrosion rates was published in reference [31]. Static simple immersion test shows the effect of time on the degradation rate. Bare MZX magnesium alloy demonstrated very low corrosion resistance in simulated body fluid (SBF) solution as shown in Figure 3. Surface oxidizing treatment increased corrosion resistance by nearly a factor of 6. However, it still corrodes too fast from an absorbable stent point of view. Biodegradable polymer coated magnesium alloy showed a reasonable corrosion rate. It seems that a thin layer of ceramic coating could be protecting the corrosion in a period of time as an example in Figure 1.

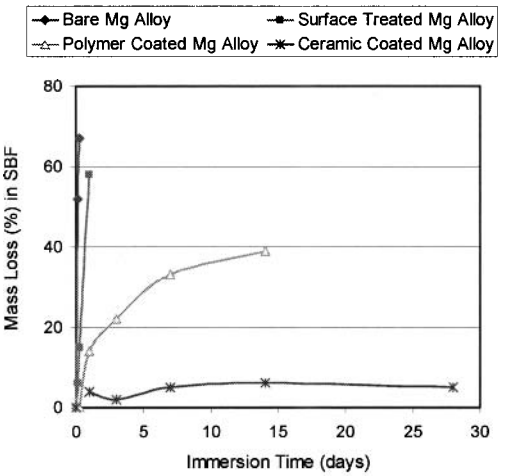

Figure 3. Mass loss of bare and surface coated magnesium alloy stents in SBF solution at 37 °C.

Potentiodynamic polarization curve gives an idea about corrosion behavior and a rapid estimation of initial corrosion rate. The polarization testing was performed in general accordance with ASTM F2129 "Standard Test Method for Conducting Cyclic Potentiodynamic Polarization Measurements to Determine the Corrosion Susceptibility of Small Implant Devices". One aim of electrochemical testing is to identify the similarity of body fluids in order to understand the correlation between in vitro and in vivo magnesium degradation. Potentiodynamic polarization of bare magnesium stents in different media are exhibited in Figure 4.

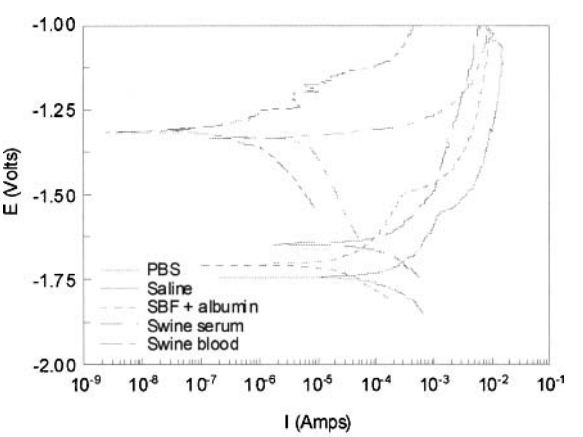

Figure 4. Potentiodynamic polarization measurements of magnesium alloy stents in different media with SCE reference electrode in Saline and PBS, and Ag/AgCl reference electrode for the other media.

Surface passivation was observed in both phosphate buffered saline (PBS) and SBF solution due to the formation of a phosphate layer. The rest potentials were higher in swine fluids than in simulated body fluids. This indicates that in vitro degradation tests in SBF are significantly different from the real degradation condition in swine fluids and perhaps in vivo. A much lower degradation rate is expected for in vivo tests than in vitro tests.

Pre-clinical results analysis

The stent implantation investigations conform to the "Guide for the Care and Use of Laboratory Animals published by the US National Institutes of Health" (NIH Publication 85–23, revised 1996). Both bare magnesium (MZX) bioabsorbable stent and platinum chromium bare metal stents (BMS) (12-mm length, 3.0-mm diameter) were implanted in the left anterior descending (LAD), left circumflex (LCX), right coronary (RCA), internal thoracic (ITA), renal and iliac arteries of female crossbred swine (Genetiporc, LLC, Alexandria, Minn). The stents were implanted at a targeted ratio of stent to artery diameter of 1.1:1.0 in the coronary arteries and 1.3:1.0 in the peripheral arteries as assessed by quantitative coronary angiography. Animals were euthanized after implant durations of 30 and 120 days.

For histology, randomly selected explanted coronary arteries were dehydrated; embedded in plastic; imaged using micro computed tomography (micro-CT); sectioned at proximal, mid, and distal stented locations and proximal and distal to the stented segment, and stained with hematoxylin and eosin and elastic trichrome stains. In selected cases, von Kossa staining was performed to confirm the presence of calcium. Morphological analysis of the in-stent sections (proximal, mid, distal) by light microscopy was performed with ordinal grading assessments of the following parameters: mural thrombus, endothelialization, strut tissue coverage, para-strut leukocytes, disruption of the internal elastic lamina (IEL), disruption of the external elastic lamina (EEL), and medial smooth muscle cell (SMC) loss.

At 30 days, neointimal thickness and percent stenosis were higher in all arteries implanted with MZX when compared to the single BMS device. Additional observations included an irregular distribution/distortion/cramping of struts in the neointima, irregularity of neointima thickness, and arterial wall calcifications in all arteries implanted with MZX devices. These findings were not observed in the control BMS stent (Figure 5). At 120 days, near complete absorption of the MZX was observed; any remaining fragments were well incorporated and covered by neointima. These fragments were surrounded either by cells (macrophages, monocytes or multinucleated giant cells) or by matrix with some calcifications (Figure 6).

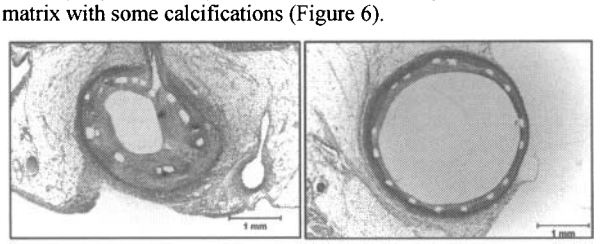

Figure 5. 30-day follow-up. Left - Histopathology of MZX vessel. Right - Histopathology of BMS vessel.

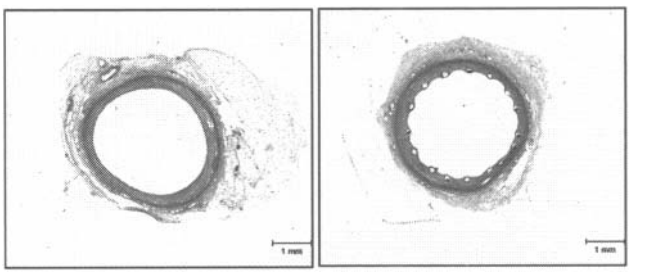

Figure 6. 120-day follow-up. Left - Histopathology of MZX vessel. Right - Histopathology of BMS vessel.

Magnesium stents demonstrated limited parastrut inflammation, absence of thrombi, and complete endothelial cell coverage similar to the bare metal control at 30 days. Lumen surface irregularities, late strut malaposition/staggering, mineralization, and reduced EEL area were observed in almost all magnesium stents in all vessel types at 30 days. These observations indicate the stents are exhibiting weakened radial strength by 30 days. All above mentioned changes may be related to the fragility of stents due to fast degradation. The discontinuity of struts can cause arterial wall damage and consequent dystrophic calcification. The fact that distortion of the stent struts coexists with mineralization suggests that it is not a result of the stents "handling" during explantation at necropsy but, most likely, the result of degradation of MZX which was quite prominent at 30 days. Arteries stented with magnesium stents have been reported in the literatures to have smaller diameters at follow-up; reduced diameters been attributed to negative remodeling [8] or recoil due to loss in radial strength [10].

Analysis of explanted stents

Conventional analytical methods can be used to characterize the condition of the magnesium stent implant after it has been harvested from the animal. It is of interest to examine the transformation of the stent metal to its by-products during degradation and to see how those products are distributed within the arterial wall. A method used to qualitatively characterize the progression of degradation is to make light microscopy examinations of stented arteries in cross-sections. Explanted stented arteries are cast in a translucent epoxy resin. Transverse sections are cut from in-stent regions (e.g., proximal, middle, distal). The wafer sections are cast in translucent metallography epoxy resin within molds to make sample configurations that can be ground and polished to prepare a metallographically smooth surface. The prepared planes are imaged with an optical stereozoom microscope and optical metallography microscope.

This technique allows for observations to be made with regard to the condition of stent struts within the artery wall and the distribution of metal degradation products. The cross-sections are first examined at relatively low magnification with an optical stereozoom microscope to see the entire stent strut ring and artery wall (Figure 7). An optical metallograph is used to examine individual struts in more details (Figures 8).

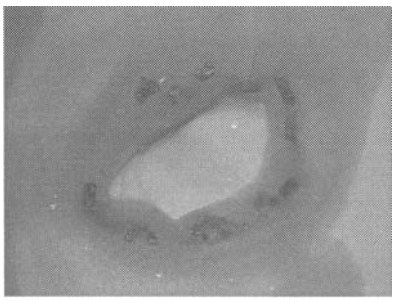

Figure 7. Optical stereozoom digital image of transverse cross section through a magnesium-stented artery. At 30 days time point, the stent struts are still present and there are degradation products adjacent to the struts.

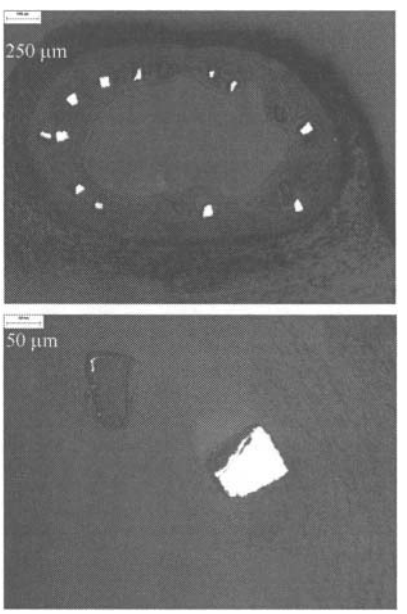

Figure 8. Optical metallograph image of a transverse cross-section through a magnesium-stented artery. The stent lumen and artery wall are visible in the top image. The remaining metal struts (white) and degradation products (grey around metal struts) can be seen in a higher magnification in the bottom. The strut next to it appears to be nearly completely degraded (dark grey).

The prepared cross-sections can then be imaged in the scanning electron microscope (SEM) in order to further resolve degraded strut features (Figure 9). The SEM image grey-scale contrast is related to the atomic number of the elements present in the features in the strut and tissue, so the degradation product can be more readily distinguished from the strut metal than with the optical microscopes. Energy dispersive spectroscopy analysis (EDS) can be used to qualitatively identify the elements that are present in the strut and degradation products. The EDS results can be mapped on the SEM image to show the distribution of elements.

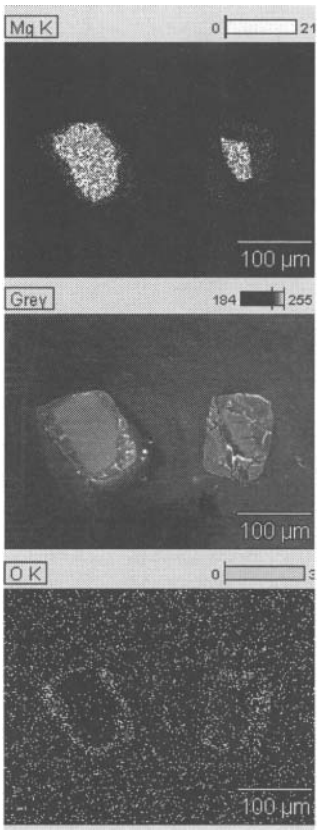

Figure 9. SEM-EDS elemental maps for magnesium (Mg, top) and oxygen (O, bottom) from two struts and their degradation products in a transverse cross-section through a magnesium-stented artery. The grey image (middle) is the SEM image that corresponds to the metal (light grey) and degradation product (dark grey).

Correlation in vivo and in vitro

The aim of a correlation is to predict in vivo outcomes through in vitro testing. Instead of running various costly animal studies, in vitro degradation studies can be used to preselect concepts ideally in a more timely manner. The experimental work included a comparison of measured mass loss values on explants (vessel containing implanted stent) with in vitro mass loss results from corrosion tests on stents. A non-destructive test procedure was developed using epoxy resin embedded vessel explants as test material and x-ray micro computed tomography (micro-CT) as analyzing method. The mass loss can be derived from the known magnesium alloy density and the micro-CT measured volume of the non-corroded stent metal. The deviation of the method depends from various parameters but mostly from pixel resolution, signal-to-noise ratio, bit depth of reconstructed image slices, strut position to beam line and polychromatic x-ray spectrum related artifacts (beam hardening).

Qualitative micro-CT assessment of magnesium stents, explanted from an animal internal thoracic artery (ITA) after 30 days, demonstrates advanced material corrosion which leads to low

stent radial strength. The magnesium stent illustrated in the top of Figure 10 has numerous discontinuous struts which have led to the stent radially collapsing from vascular motion. Qualitative micro-CT assessment also shows magnesium stents do not corrode uniformly but rather focally, with corrosion generally initiating in high-strain regions. Quantitative mass loss measurements can be made by imaging stents of known mass (Figure 10 bottom) along with stents implanted during an in vivo study. The purpose of imaging stents of known mass is to determine an appropriate micro-CT threshold factor signifying the difference between magnesium and epoxy resin/tissue.

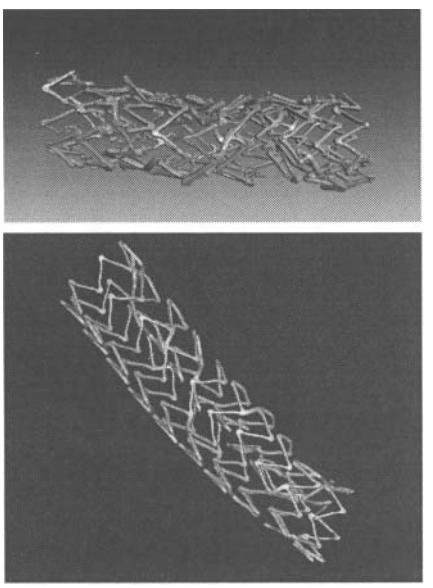

Figure 10. A magnesium alloy stent explanted from ITA after 30 days (top). A known mass stent implanted in epoxy resin (bottom).

Since the in vitro mass loss test is accelerated compared to in vivo mass loss, a more complex approach has to be used to determine corrosion as shown in Figure 11. Relative mass loss determined through in vitro test is fitted into a curve over different time points. The relative mass loss determined through measurement on explants is then found in this curve and related to a time point on the in vitro time axis. This is done for every time point from explants that creates a correlation curve between in vitro and in vivo time points as shown in the upper right part of Figure 11. Detailed correlation experiments are ongoing and will be published elsewhere.

Conclusion

Magnesium alloys have reduced mechanical strength relative to conventional metal stent materials, but the amount of strength required and stent designs to maintain stent diameters over a certain time frame is relatively unknown. Magnesium alloy stents provide a suitable corrosion rate in the physiologic environment with surface coating. Magnesium is an essential mineral for human metabolism which is a plus for bioabsorbable stent material.

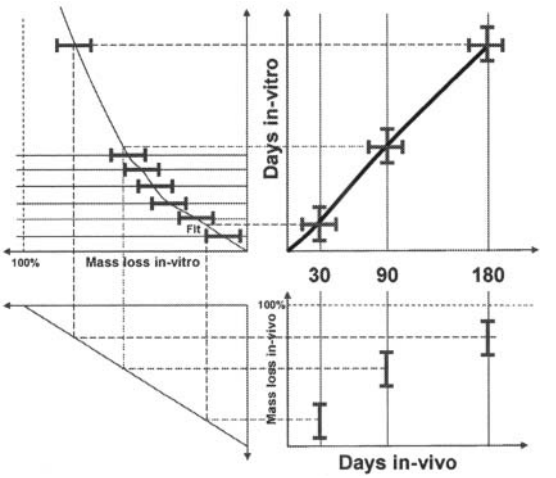

Figure 11: In-vitro / in-vivo correlation.

Intravascular ultrasound analysis at the termination of the 120-day animal provided no evidence of remaining stent material in the treated area of the vessels; histology confirmed nearly complete absorption within 120 days of implantation. At both 30 and 120 days post implantation, vascular response of coronary and peripheral arteries demonstrated absence of thrombi, complete strut coverage and minimal parastrut inflammation in all arteries implanted with either magnesium alloy or BMS devices. There was no evidence of myocardial abnormalities of any kind at 30 and 120 days. Evidence of negative remodeling at 30 days and positive at 120 days was noted by angiography and intervascular ultrasound (IVUS) at termination.

Both in vitro and preclinical in vivo data suggest that delayed and more uniform corrosion of the stent material is required. The vessel requires strength for a longer period of time than 30 days to allow for the completion of vessel healing. Therefore, new alloys and corrosion protection schemes such as coatings may be beneficial in generating a more complete understanding of the design requirements of magnesium alloy stents. In vitro experiments inherently exhibit a direct correlation to the real case, whereas a direct simulation of the in vivo case seems feasible.

References

1. J. E. Moore, J. S. Soares, and K. R. Rajagopal, "Biodegradable Stents: Biomechanical Modeling Challenges and Opportunities", *Cardiovascular Engineering and Technology*, 1 (1) (2010), 52-65.
2. R. Jabara, L. Pendyala, J. Chen, and N. Chronos, "Bioabsorbable Stents: The Future Is Near", *Cardiac Interventions Today*, June/July (2009), 50-53.
3. P. Erne, M. Schier, and T. J. Resink, "The Road to Bioabsorbable Stents: Reaching Clinical Reality?", *Cardiovas Intervent Radiol*, 29 (2006), 11-16.
4. G. Mani, M. D. Feldman, D. Patel, and C. M. Agrawal, "Coronary Stents: A Materials Perspective", *Biomaterials*, 28 (2007) 1689-1710
5. H. Hermawan, M. Moravej, D. Dube, M. Fiset, and D. Mantovani, "Degradation Behaviour of Metallic Biomaterials

for Degradable Stents", *Advanced Materials Research*, 15-17 (2007), 113-118.
6. C. Di Mario, H. Griffiths, O. Goktekin, N. Peeters, J. Verbist, M. Bosiers, K. Deloose, B. Heublein, R. Rohde, V. Kases, C. Ilsley, and R. Erbel, "Drug-Eluting Bioabsorbable Magnesium Stent", *J, Interventional Cardiology*, 17 (6) (2004), 391-395.
7. B. Heublein, R. Rohde, V. Kaese, M. Niemeyer, W. Hartung, and A. Haverich, "Biocorrosion of Magnesium Alloy: A New Principle in Cardiovascular Implant Technology?" *Heart*, 89 (2003), 651-656.
8. M. Maeng, L. O. Jensen, E. Falk, H. R. Andersen, and L. Thuesen, "Negative Vascular Remodelling after Implanttation of Bioabsorbable Magnesium Alloy Stents in Porcine Coronary Arteries: A Randomised Comparison with Bare-metal and Sirolimus-eluting Stents", *Heart*, 95 (2009), 241-246.
9. R. Waksman, R. Pakala, P. K. Kuchulakanti, R. Baffour, D. Hellinga, R. Seabron, F. O. Tio, E. Wittchow, S. Hartwig, C. Harder, R. Rohde, B. Heublein, A. Andreae, K. Waldmann and A. Haverich, "Safety and Efficacy of Bioabsorbable Magnesium Alloy Stents in Porcine Coronary Arteries", *Catheterization and Cardiovascular Intervention*, 68 (2006), 607-617.
10. T. L. Pinto Slottow, R. Pakala, T. Okabe, D. Hellinga, R. J. Lovec, F. O. Tio, A. B. Bui, and R. Waksman, "Optical Coherence Tomography and Intravascular Ultrasound Imaging of Bioabsorbable Magnesium Stent Degradation in Porcine Coronary Arteries", *Cardiovascular Revascularization Medicine*, 9 (2008), 248-254.
11. P. Peeters, M. Boisers, J. Vernist, K. Deloose, and B. Heublein, "Preliminary Results after Application of Absorbable Metal Stents in Patients with Critical Limb Ischemia", *J Endovasc Ther*, 12 (2005), 1-5.
12. R. Erbel, C. Di Mario, J. Bartunek, J. Bonnier, B. De Bruyne, F. Eberli, P. Erne, M. Haude, B. Heublein, M. Horrigan, C. Ilsley, D. Bose, J. Koolen, T. F. Luscher, N. Weissman, and R. Waksman, "Temporary Scaffolding of Coronary Arteries with Bioabsorbable Magnesium Stent: A Prospective, Non-randomised Multicentre Trial", *The Lancet* 369 (2007), 1869-1875.
13. R. Waksman, R. Erbel, C. Di Mario, J. Bartunek, B. de Bruyne, F. R. Eberli, P. Erne, M. Haude, M. Horrigan, C. Ilsley, D. Bose, H. Bonnier, J. Koolen, T. F. Luscher, and N. J. Weissman, "Early- and Long-Term Intravascular Ultrasound Angiographic Findings After Bioabsorbable Magnesium Stent Implantation in Human Coronary Arteries", *JACC Cardiovascular Interventions* 2 (4) (2009), 312-320.
14. X. N. Gu and Y. F. Zheng, "A Review on Magnesium Alloys as Biodegradable Materials", *Front. Mater. Sci. China*, 4 (2) (2010), 111-115.
15. X. Gu and Y. Zheng, "In Vitro Corrosion and Biocompatibility of Binary Magnesium Alloys", *Biomaterials*, 30 (2009), 484-498.
16. B. Zberg, P. J. Uggowitzer, and J. F. Löffler, "MgZnCa GlassesWithout Clinically Observable Hydrogen Evolution for Biodegradable Implants", *Nature Materials*, 8 (11) (2009), 887-891.
17. A. C. Hanzi, F. H. Dalla Torre, A. S. Sologubenko, P. Gunde, R. Schmid-Fetzer, M. Kuehlein, J. F. Löffler, and P. J. Uggowitzer, "Design Stategy for Microalloyed Ultra-ductile Magnesium Alloys", *Philosophical Magazine Letters*, 89 (6) (2009), 377-390.
18. A. C. Hanzi, P. Gunde, M. Schinhammer, and P. J. Uggowitzer, "On the Biodegradation Performance of an Mg-Y-Re Alloy with Various Surface Conditions in Simulated Body Fluid", *Acta Biomaterialia*, 5 (2009), 162-171.
19. J. G. Brumer, R. Hahn, J. Kunze, and S. Virtanen, „Porosity Tailored Growth of Black Anodic Layers on Magnesium in an Organic Electrolyte", *J. Electrochem. Soc.*, 156 (2) (2009), C62-C66.
20. R. Rettig and S. Virtanen, "Composition of Corrosion Layers on a Magnesium Rare-earth Alloy in Simulated Body Fluids", *J. Biomed Mater Res A*, 88 (2) (2009), 359-369.
21. R. Rettig and S. Virtanen, "Time-dependent Electrochemical Characterization of the Corrosion of a Magnesium Rare-earth Alloy in Simulated Body Fluids", *J. Biomed Mater Res A*, 85 (1) (2008), 167-175.
22. F. Witte, "The History of Biodegradable Magnesium Implants: A Review", *Acta Biomaterialia*, 6 (2010), 1680-1692.
23. N. Hort, Y. Huang, D. Fechner, M. Stormer, C. Blawert, F. Witte, C. Vogt, H. Drucker, R. Willumeit, K. U. Kainer, and F. Feyerabend, "Magnesium Alloy as Implant Materials – Principles of Property Design for Mg-Re Alloys", *Acta Biomaterialia*, 6 (2010), 1714-1725.
24. C. Janning, E. Willbold, C. Vogt, J. Nellesen, A. Meyer-Lindenberg, H. Windhagen, F. Thorey, and F. Witte, "Magnesium Hydroxide Temporarily Enhancing Osteoblast Activity and Decreasing the Osteoclast Number in Peri-implant Bone Remodelling", *Acta Biomaterialia*, 6 (2010), 1861-1868.
25. F. Witte, J. Fischer, J. Nellesen, C. Vogt., T. Donath, and F. Beckmann, "In vivo Corrosion and Corrosion Protection of Magnesium Alloy LAE442", *Acta Biomaterialia*, 6 (5) (2010), 1792-1799.
26. F. Feyerabend, J. Fischer, J. Holtz, F. Witte, R. Willumeit, H. Drucker, C. Vogt, and N. Hort, "Evolution of Short-term Effects of Rare Earth and Other Elements Used in Magnesium Alloys on Primary Cells and Cell Lines", *Acta Biomaterialia*, 6 (5) (2010), 1834-1842.
27. F. Witte, J. Fischer, J. Nellesen, H-A. Crostack, V. Kaese, A. Pisch, F. Beckmann, and H. Windhagen, "In Vitro and In Vivo Corrosion Measurements of Magnesium Alloys", *Biomaterials*, 27 (2006), 1013-1018.
28. W. D. Muller, M. L. Nascimento, M. Zeddies, M. Corsico, L. M.Gassa, and M. A. F. L. de Mele, "Magnesium and Its Alloys as Degradable Biometerials, Corrosion Studies Using Potentiodynamic and EIS Electrochemical Techniques", *Materials Research*, 10 (1) (2007), 5-10.
29. Y. Yun, Z. Dong, N. Lee, Y. Liu, D. Xue, X. Guo, J. Kuhlmann, A. Doepke, H. B. Haslsall, W. Heinemann, S. Sundaramurthy, M. J. Schulz, Z. Yin, V. Shanov, D. Hurd, P. Nagy, W. Li, and C. Fox, "Revolutionizing Biodegradable Metals", *Materials Today*, 12 (10) (2009), 22-32.
30. M. B. Kannan and R. K. S. Raman, "In Vitro Degradation and Mechanical Integrity of Calcium-Containing Magnesium Alloys in Modified-Simulated Body Fluid", *Biomaterials*, 29 (2008), 2306-2314.
31. N. T. Kirkland, J. Lespagnol, N. Birbilis, and M. P. Staiger, "A Survey of Bio-corrosion Rates of Magnesium Alloys", *Corrosion Science*, 52 (2010), 287-291.